Heteroatom Chemistry
Volume 1, Number 1, 1990

Crystallographic Analysis of Thermochromic, Unsolvated Tetramesityldisilene at 173 K and 295 K

Brian D. Shepherd, Charles F. Campana,† and Robert West*

Department of Chemistry, University of Wisconsin, Madison, Wisconsin 53706 U.S.A.

Received 27 December 1988.

ABSTRACT

X-ray crystal structure determinations of tetramesityldisilene (**1**) *at 295 K, where it is bright orange, and at 173 K, where it is pale yellow, were experimentally equivalent. The thermochromism of* **1**, *therefore, is not due to changes in conformation; a vibrational origin is considered. The crystal structure of unsolvated* **1** *differs substantially from that of the toluene solvate* (**1**·C_7H_8) *because of different crystal packing of the two forms. These two solid-state structures are compared with those of four other disilenes.*

Tetramesityldisilene (**1**) was the first example of an isolable disilene, a long-sought type of compound [1, 2]. The x-ray crystal structure of **1** in unsolvated form has not previously been reported, but the crystal structure of **1** solvated with toluene (**1**·C_7H_8) [3] was published in 1983 [4]. In this early work the thermochromic behavior of **1** in the solid state was also noted.

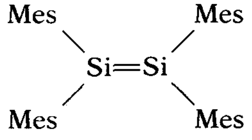

1

where Mes = 2,4,6-trimethylphenyl.

THERMOCHROMISM

Unsolvated tetramesityldisilene (**1**) is a bright orange solid at room temperature but turns pale yellow when cooled below −50°C. On heating the color becomes more intense, and the sample melts at 196°C to a red liquid. The solvated compound (**1**·C_7H_8) is a yellow solid both at room temperature and below, but when heated **1**·C_7H_8 darkens to orange and then melts to a red liquid at 178°C. Other tetraaryldisilenes are also thermochromic [5], as is a silaimine (contains Si=N) [6], a digermene (contains Ge=Ge) [7], and a germene (contains Ge=C) [8].

Earlier, we speculated that the thermochromism of disilenes might result from conformational changes around the silicon–silicon double bond [2]. It has been suggested that the thermochromism of tetrakis[bis(trimethylsilyl)methyl]-distannene in the solid state may be conformational in origin [9, 10]. The visible color of disilenes arises from the π–π^* transition of the silicon–silicon double bond, which falls near 400 nm. This transition energy should be sensitive to distortions at the Si=Si bond. Theoretical calculations on $H_2Si{=}SiH_2$ and $(CH_3)_2Si{=}Si(CH_3)_2$ indicate that the potential energy surface is quite flat for both anti pyramidalization of the silicon atoms and for twisting about the Si–Si axis [11]. It seemed reasonable that the structure of such unconstrained molecules might change with temperature and so alter the π–π^* excitation energy. Similar thermochromism, involving bathochromic shifts of π–π^* excitations with increasing temperature, has been observed for hindered olefins and attributed to twisting of the C=C double bond [12]. The transition energy in disilenes may also be influenced by

---

[*] To whom correspondence should be addressed.

[†] Current address: Siemens Analytical X-Ray Instruments, Inc., Madison, Wisconsin 53711 U.S.A.

1042-7163/90/$1.00 + .25

conjugation between aromatic ring and Si=Si π orbitals. The degree of conjugation would depend on the angle of rotation of these rings with respect to the Si=Si bond, which might also be temperature dependent.

We have now determined the crystal structure of unsolvated **1**, both at 22°C, where it is orange, and at −100°C, where it is pale yellow. The two structures were identical within experimental error [13], and on this basis we conclude that the thermochromic behavior in crystalline tetramesityldisilene (**1**) does not arise from changes in conformation or from any other structural change. The disilene chromophores on neighboring molecules are well separated in the solid state structure of **1**, so intermolecular interactions are not likely to be associated with the thermochromism; moreover the packing does not change between 22 and −100°C. The thermochromism does not seem to result from an electronically active impurity, because the thermochromic behavior persists in highly purified samples and, indeed, is largely independent of the degree of purity of **1**.

A possible explanation is that the visible absorption band broadens as the sample is heated because of a change in the distribution of molecules among the vibrational levels of the ground state; a frequency shift may accompany the broadening. This concept was developed previously to account for the thermochromism in solution of a number of anthrones and thiocarbonyl compounds [14]. If this "hot-band" effect is responsible for the thermochromism of **1**, however, it must be due to a vibration that is present only in the solid, because **1** shows no thermochromism in solution. Possibly **1** relaxes in solution to a conformation in which the active molecular vibration in unimportant.

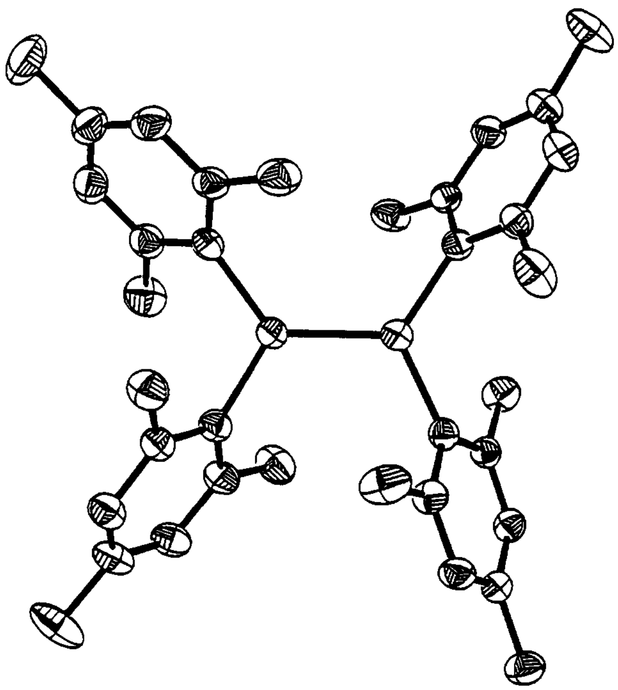

FIGURE 1 50% Thermal ellipsoid drawing of unsolvated **1**. Hydrogen atoms have been omitted for clarity.

TABLE 1 Bond Lengths in Unsolvated **1** at −100°C

Bond	*Bond length* (Å) (*SD*)[a]	*Bond*	*Bond length* (Å) (*SD*)[a]
Si1–Si2	2.143 (2)	Si1–C1	1.886 (4)
Si1–C10	1.869 (5)	Si2–C19	1.867 (5)
Si2–C28	1.892 (4)	C1–C2	1.406 (6)
C1–C6	1.395 (6)	C2–C3	1.384 (7)
C2–C7	1.511 (7)	C3–C4	1.388 (7)
C4–C5	1.377 (8)	C4–C8	1.514 (7)
C5–C6	1.406 (6)	C6–C9	1.500 (7)
C10–C11	1.420 (6)	C10–C15	1.407 (8)
C11–C12	1.377 (7)	C11–C16	1.514 (9)
C12–C13	1.387 (9)	C13–C14	1.391 (6)
C13–C17	1.500 (8)	C14–C15	1.381 (7)
C15–C18	1.511 (6)	C19–C20	1.411 (6)
C19–C24	1.414 (6)	C20–C21	1.377 (7)
C20–C25	1.511 (6)	C21–C22	1.383 (6)
C22–C23	1.385 (7)	C22–C26	1.500 (8)
C23–C24	1.390 (7)	C24–C27	1.515 (7)
C28–C29	1.409 (7)	C28–C33	1.403 (7)
C29–C30	1.383 (5)	C29–C34	1.512 (7)
C30–C31	1.382 (7)	C31–C32	1.377 (7)
C31–C35	1.507 (5)	C32–C33	1.394 (5)
C33–C36	1.507 (9)		

[a] Estimated standard deviations are in parentheses.

Detailed analysis of the vibrational and electronic spectra in the solid state may be quite useful, both for **1** and for the other multiply bonded main-group compounds that show thermochromism.

STRUCTURAL COMPARISON

Unsolvated and Solvated 1

The crystal structures of **1** and **1**·C_7H_8 differ dramatically. Shown in Figure 1 is a 50% thermal ellipsoid drawing of unsolvated tetramesityldisilene (**1**); bond lengths and angles at −100°C are given in Tables 1 and 2 (the numbering scheme for **1** is shown in Figure 2). The two forms crystallize in different space groups with different site symmetries. Some structural parameters in **1** and **1**·C_7H_8 are listed in Table 3 with values from other disilenes (discussed below). In **1**·C_7H_8, a crystallographic twofold rotation axis is present in the plane of the silicon and attached carbon atoms, bisecting the Si=Si double bond. The toluene (disordered) lies on this axis between the aromatic rings, as shown in the packing plot of Figure 3; Figure 4 is the corresponding plot for unsolvated **1**. The shortest carbon–carbon contact, 373 pm, between the

TABLE 2 Bond Angles (°) in Unsolvated **1** at −100°C

Bonds	Angle (°) (*SD*)[a]	Bonds	Angle (°) (*SD*)[a]
Si2–Si1–C1	126.7 (2)	Si2–Si1–C10	119.5 (1)
C1–Si1–C10	112.1 (2)	Si1–Si2–C19	121.2 (1)
Si1–Si2–C28	115.4 (2)	C19–Si2–C28	121.5 (2)
Si1–C1–C2	117.6 (3)	Si1–C1–C6	123.6 (3)
C2–C1–C6	118.6 (4)	C1–C2–C3	120.2 (4)
C1–C2–C7	122.0 (4)	C3–C2–C7	117.8 (4)
C2–C3–C4	121.4 (5)	C3–C4–C5	118.5 (4)
C3–C4–C8	119.8 (5)	C5–C4–C8	121.6 (5)
C4–C5–C6	121.3 (5)	C1–C6–C5	119.8 (4)
C1–C6–C9	122.5 (4)	C5–C6–C9	117.7 (4)
Si1–C10–C11	121.6 (4)	Si1–C10–C15	120.5 (3)
C11–C10–C15	117.8 (4)	C10–C11–C12	119.3 (5)
C10–C11–C16	121.9 (5)	C12–C11–C16	118.7 (4)
C11–C12–C13	123.2 (4)	C12–C13–C14	117.0 (5)
C12–C13–C17	120.4 (4)	C14–C13–C17	122.6 (6)
C13–C14–C15	121.8 (5)	C10–C15–C14	120.7 (4)
C10–C15–C18	120.6 (4)	C14–C15–C18	118.7 (5)
Si2–C19–C20	122.7 (3)	Si2–C19–C24	119.1 (3)
C20–C19–C24	118.0 (4)	C19–C20–C21	119.8 (4)
C19–C20–C25	122.6 (4)	C21–C20–C25	117.5 (4)
C20–C21–C22	122.6 (4)	C21–C22–C23	117.7 (5)
C21–C22–C26	120.3 (4)	C23–C22–C26	121.9 (4)
C22–C23–C24	121.8 (4)	C19–C24–C23	119.9 (4)
C19–C24–C27	121.4 (4)	C23–C24–C27	118.6 (4)
Si2–C28–C29	121.0 (3)	Si2–C28–C33	120.2 (4)
C29–C28–C33	118.5 (4)	C28–C29–C30	119.9 (4)
C28–C29–C34	121.8 (3)	C30–C29–C34	118.3 (5)
C29–C30–C31	122.0 (5)	C30–C31–C32	118.0 (4)
C30–C31–C35	121.6 (5)	C32–C31–C35	120.3 (4)
C31–C32–C33	122.1 (5)	C28–C33–C32	119.5 (5)
C28–C33–C36	123.5 (4)	C32–C33–C36	116.9 (5)

[a] Estimated standard deviations are in parentheses.

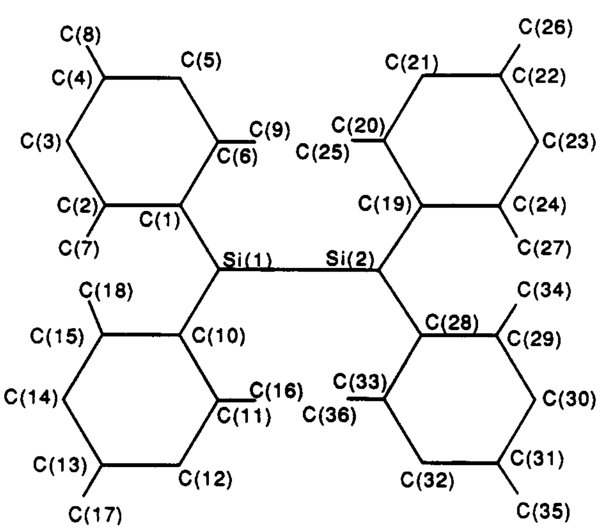

FIGURE 2 Numbering scheme for **1**.

toluene solvate and the disilene involves a meta-carbon of the toluene and an *ortho*-methyl carbon of the mesityl substituent. The Si=Si bond is slightly elongated to accomodate the orientations of the aromatic rings that are imposed by the toluene, but the perturbation does not cause widening of the Si–Si–C angles. In the absence of toluene, no crystallographic symmetry element is present and the Si=Si double bond is less twisted [15] and the silicon atoms are less pyramidal [16] in unsolvated **1**. The influence of the toluene on the overall structure is substantial (compare the packing plots in Figures 3 and 4) and all of the pertinent parameters

TABLE 3 Structural Parameters in Disilenes

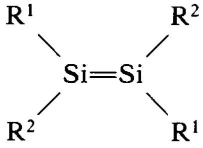

Disilene	*R*¹ [a]	*R*² [a]	*T* (°C)	*Space group*	*Site symm.*	*Z*	$r_{Si=Si}$ (*pm*)	*Twist*[b] (°)	*Pyram.*[c] (°)	*Ring orient.*[d] (°)
1a	Mes	Mes	−100	$P2_1/c$	C_1-1	4	214.3 (2)	3	12, 14	42, 52, 67, 70
1b	Mes	Mes	22	$P2_1/c$	C_1-1	4	213.8 (2)	3	10, 13	43, 52, 66, 69
1·C_7H_8	Mes	Mes	−85	$I4_1/a$	C_2-2	8	216.0 (1)	12[e]	18	35, 35, 78, 78
2	DEP	DEP	nr[f]	*Pcnb*	C_2-2	4	214.0 (3)	10	0	62, 62, 64, 64
3	Is	Is	nr[f]	$P\bar{1}$	C_1-$\bar{1}$	2	214.4 (nr[f])	3	0	52, 56, 58, 61
4	Mes	*t*-Bu	25	$P\bar{1}$	C_i-$\bar{1}$	1	214.3 (1)	0	0	88, 88
5	Mes	Ad	22	$P\bar{1}$	C_i-$\bar{1}$	1	213.6 (3)	0	3	87, 87

[a] Mes = 2,4,6-trimethylphenyl; DEP = 2,6-diethylphenyl; Is = 2,4,6-triisopropylphenyl; Ad = 1-adamantyl.
[b] Ref. [15].
[c] Ref. [16].
[d] Angle between the aromatic ring plane and the corresponding C_{aryl}–Si–Si plane.
[e] Ref. [19].
[f] Not reported.

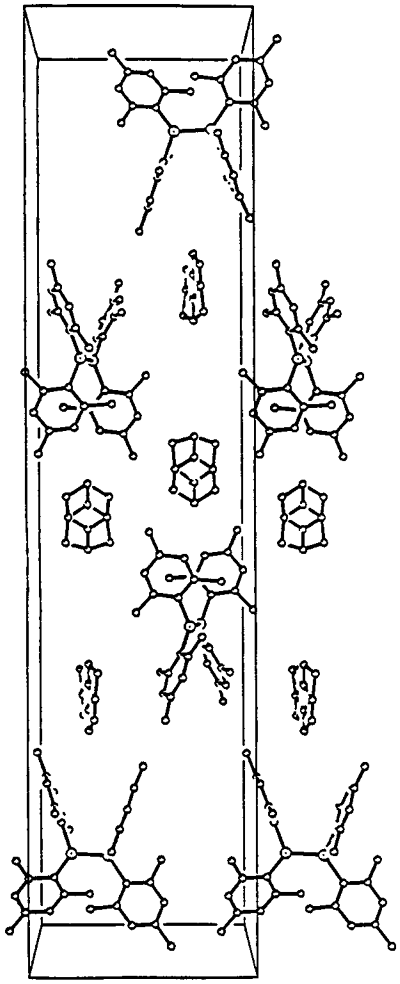

FIGURE 3 Packing plot for $1 \cdot C_7H_8$ along the *a* axis (the toluene is in twofold-disordered positions, as shown).

are affected (Table 3) due to different crystal packing in the two forms.

Other Disilenes

x-Ray crystal structures have also been determined for tetrakis(2,6-diethylphenyl)disilene (**2**) [17], tetrakis(2,4,6-triisopropylphenyl)disilene (**3**) [5a], *E*-1,2-di-*t*-butyldimesityldisilene (**4**) [4b], and *E*-1,2-di(1-adamantyl)dimesityldisilene (**5**) [18] (Table 3). Except for $1 \cdot C_7H_8$, which has $r_{Si=Si}$ 216.0 ± 0.1 pm, the disilenes all show Si═Si distances within 0.4 pm of 214.0 pm, which is about 20 pm shorter than the normal Si—Si single bond length.

The disilenes in the solid state possess different crystallographic symmetry elements, previously mentioned for **1** and $1 \cdot C_7H_8$. Molecules of **2**, like those of $1 \cdot C_7H_8$, have a crystallographic twofold symmetry axis that bisects the Si═Si bond. The 1,2-dialkyldiaryldisilenes (**4** and **5**) contain a center of symmetry midway between the silicon atoms. In these disilenes ($1 \cdot C_7H_8$, **2**, **4**, and **5**) only half of the molecule is crystallographically independent, so there is only one kind of silicon atom and two sets of substituents. We believe that the structure obtained for $1 \cdot C_7H_8$, **4**, and **5** with crystallographic symmetry elements are the exact, not the average, configurations, because the thermal ellipsoids show no unusual enlargement. This possibility was not addressed in the report on the solid state structure of **2** [17]. No such symmetry element is present in **1** or **3** so each silicon atom in these disilenes is independent, as is each of the four substituents, and the obtained structure is presumably the instantaneous structure.

The structural arrangement at the Si═Si double bond ranges from planar to twisted and pyramidal [15, 16]. In **4**, the two silicon and four attached carbon atoms are coplanar, just as in a normal olefin structure. The silicon atoms in **5**, however, are slightly pyramidal (3°). In **2** and **3**, the arrangement at each silicon atom is coplanar, but the two halves of the molecule are twisted by 10° in **2** and by 3° in **7**. Deviation from planarity in **1** consists of a small twist (3°) of the double bond and anti pyramidalization (12° at one silicon atom and 14° at the other). In contrast, the silicon atoms in $1 \cdot C_7H_8$ are more pyramidal (18°) and there is more twisting of the double bond (12°) [19]. Distortions

FIGURE 4 Packing plot for unsolvated **1** along the *b* axis.

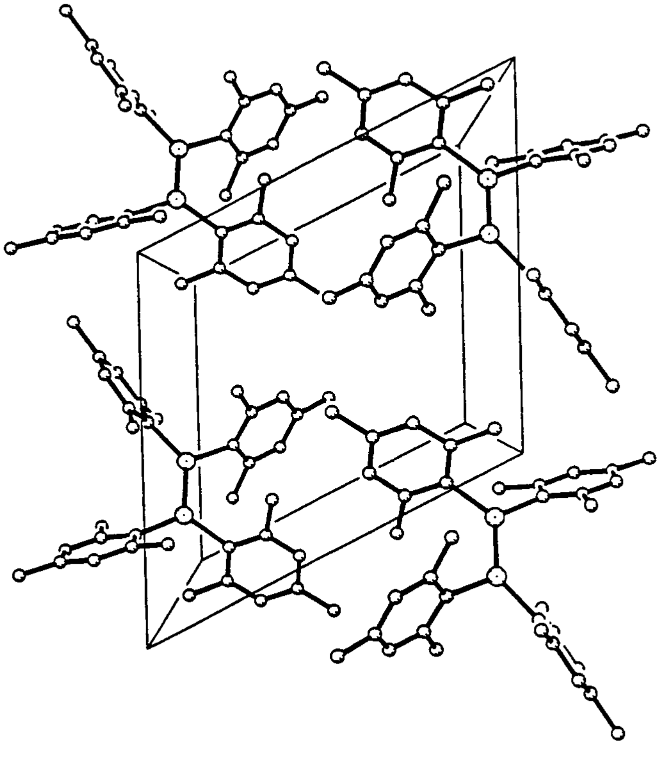

in sterically crowded olefins also consist of twisting and pyramidalization [20].

The deviations of disilenes from planar geometry are consistent with the previously mentioned theoretical calculations on $H_2Si{=}SiH_2$ and $(CH_3)_2Si{=}Si(CH_3)_2$, which indicates that the Si=Si double bond is quite malleable [10]. The differences in structure around the double bond may be due to crystal packing forces and steric constraints.

The aromatic rings in all the disilenes are rotated relative to the respective C_{aryl}–Si–Si plane. In **4** and **5**, the mesityl rings are inclined at angles of 88° and 87°, respectively, essentially orthogonal to the Si=Si double bond. In **1**·C_7H_8, two of the rings, cis to each other, are more nearly orthogonal (78° angle), whereas the other two are more nearly coplanar (35° angle) with the silicon framework. In unsolvated **1** the rings are in similar orientations, with one cis pair more orthogonal (67° and 70° rotations) and the other pair less orthogonal (42° and 52° rotations), but the angles are not as extreme as in **1**·C_7H_8 [21]. In **3**, the particular arrangement of the aromatic rings (rotation angles 52°, 56°, 58°, and 61°) is probably caused by meshing of neighboring *ortho*-isopropyl groups. In **2**, the rings are rotated by 62° and 64°.

Electronic interaction between the aryl and Si=Si π systems is dependent on the orientation of the aromatic rings [22], and this is reflected in the UV–visible absorption spectra that are obtained in solution. The lowest energy electronic absorption for **4** and **5**, which have no aryl groups in a position suitable for conjugation with the Si=Si bond [23], is at 390–400 nm [24], similar to the λ_{max} recorded for many tetraalkyldisilenes [25]. In the tetraaryldisilenes, where conjugation between the aryl and Si=Si π systems is possible, λ_{max} occurs near 420 nm. In the solid state, where only a qualitative assessment is possible, the absorption band for the tetraaryldisilenes is significantly red shifted compared to that of the dialkyldiaryldisilenes [26].

SUMMARY

Disilenes exhibit many variations in their solid-state structures, with different deformations of the Si=Si double bond and distinct orientations of the substituents. However, the thermochromism of crystalline, unsolvated tetramesityldisilene is due to electronic factors, not structural changes, as shown by the independence of its crystal structure with respect to temperature.

EXPERIMENTAL SECTION

Tetramesityldisilene (**1**)

This compound was prepared as previously described [4]. Orange crystals suitable for x-ray diffraction were obtained by allowing an almost saturated, hot hexane solution to cool to room temperature.

TABLE 4 Structure Determination Summary for Unsolvated **1** at −100°C

Empirical formula	$C_{36}H_{44}Si_2$
Color; habit	Orange prisms
Crystal size (mm)	0.20 × 0.30 × 0.40
Crystal system	Monoclinic
Space group	$P2_1/c$
Unit cell dimensions	a = 11.434 (2) Å[a]
	b = 28.269 (5) Å[a]
	c = 10.945 (2) Å[a]
	β = 117.119 (14)°[a]
Volume	3148.8 (11)[a]
Z	4
Formula weight	532.9
Density (calc.)	1.124 mg m^{-3}
Absorption coefficient	1.163 mm^{-1}
F(000)	1152
Diffractometer used	Nicolet P3/F
Radiation	CuKα (λ = 1.54178 Å)
2θ range	3.5–115.0°
Scan type	Wykoff
Scan speed	Variable; 3.98–29.30°/min^{-1} in w
Scan range (w)	2.00° plus Kα separation
Background measurement	Stationary crystal and stationary counter at beginning and end of scan, each for 50.0% of total scan time
Standard reflections	Three measured every 97 reflections
Index ranges	$-12 \leq h \leq 11$, $0 \leq k \leq 30$, $0 \leq l \leq 11$
Reflections collected	4552
Independent reflections	4175 (R_{int} = 3.60%)
Observed reflections	3084 [$F > 6.0\sigma(F)$]
Absorption correction	N/A
System	Nicolet SHELXTL PLUS (MicroVAX II)
Solution	Direct methods
Refinement method	Full-matrix least squares
Quantity minimized	$\Sigma w(F_0 - F_c)^2$
Absolute configuration	N/A
Extinction correction	χ = 0.0008 (5),[a] where $F^* = F[1 + 0.002\chi F^2/\sin(2\theta)]^{-1/4}$
Hydrogen atoms	Riding model, fixed isotropic U
Weighting scheme	$w^{-1} = \sigma^2(F) + 0.0016F^2$
Final R indices (observed data)	R = 6.61%, wR = 9.24%
R indices (all data)	R = 8.90, wR = 12.68%
Goodness of fit	1.88
Largest and mean Δ/σ	0.001, 0.000
Data to parameter ratio	9.0 : 1
Largest difference peak	0.41 eÅ^{-3}
Largest difference hole	−0.48 eÅ^{-3}

[a] Numbers in parentheses are standard deviations.

TABLE 5 Atomic Coordinates ($\times 10^4$) and Equivalent Isotropic Displacement Coefficients ($Å^2 \times 10^3$) for Unsolvated **1**

	x^a	y^a	z^a	$\mathbf{U}(eq)^{a,b}$
Si1	−109 (1)	1375 (1)	8919 (1)	33 (1)
Si2	−53 (1)	967 (1)	7297 (1)	33 (1)
C1	1137 (4)	1367 (2)	10,788 (5)	30 (2)
C2	1457 (5)	1800 (2)	11,494 (5)	38 (2)
C3	2236 (5)	1810 (2)	12,901 (5)	46 (2)
C4	2714 (5)	1396 (2)	13,650 (5)	45 (2)
C5	2440 (4)	972 (2)	12,957 (5)	41 (2)
C6	1671 (4)	952 (2)	11,524 (5)	32 (2)
C7	1006 (5)	2268 (2)	10,758 (6)	52 (3)
C8	3556 (6)	1422 (3)	15,190 (6)	68 (3)
C9	1448 (5)	476 (2)	10,849 (5)	44 (4)
C10	−1675 (4)	1669 (2)	8641 (5)	32 (2)
C11	−2166 (4)	2072 (2)	7780 (5)	33 (2)
C12	−3234 (5)	2310 (2)	7737 (5)	40 (2)
C13	−3860 (4)	2180 (2)	8513 (5)	37 (2)
C14	−3411 (4)	1773 (2)	9307 (5)	33 (2)
C15	−2348 (4)	1521 (2)	9376 (4)	31 (2)
C16	−1546 (5)	2250 (2)	6904 (6)	49 (2)
C17	−4953 (5)	2477 (2)	8499 (6)	57 (3)
C18	−1929 (5)	1078 (2)	10,247 (5)	39 (2)
C19	1506 (4)	690 (2)	7495 (4)	26 (2)
C20	2696 (4)	943 (2)	7965 (4)	31 (2)
C21	3831 (4)	710 (2)	8175 (5)	34 (2)
C22	3860 (5)	231 (2)	7930 (5)	36 (2)
C23	2692 (5)	−18 (2)	7461 (5)	37 (2)
C24	1525 (4)	199 (2)	7250 (5)	33 (2)
C25	2792 (5)	1467 (2)	8255 (5)	39 (2)
C26	5131 (5)	−7 (2)	8211 (6)	50 (3)
C27	298 (5)	−101 (2)	6781 (6)	46 (2)
C28	−1516 (4)	1042 (2)	5552 (5)	30 (2)
C29	−1397 (4)	1282 (1)	4488 (4)	28 (2)
C30	−2508 (4)	1387 (2)	3283 (5)	31 (2)
C31	−3754 (4)	1266 (2)	3086 (4)	31 (2)
C32	−3865 (4)	1023 (2)	4117 (5)	34 (2)
C33	−2773 (5)	906 (2)	5345 (5)	35 (2)
C34	−81 (4)	1447 (2)	4636 (5)	40 (2)
C35	−4957 (5)	1375 (2)	1762 (5)	41 (2)
C36	−3023 (5)	626 (2)	6374 (6)	50 (2)

[a] Numbers in parentheses are standard deviations.

[b] Equivalent isotropic **U** is defined as one-third the trace of the orthogonalized $\mathbf{U}_{ij}$ tensor.

X-Ray Crystallography

A crystal grown as described above was anchored on a glass fiber with cyanoacrylate glue and sealed in a glass capillary under argon. The same crystal was used at 22°C and at −100°C. A summary of the structure determination at −100°C is given in Table 4, with atomic coordinates in Table 5. The data at 22°C is in the supplementary material.

Acknowledgment

Research was sponsored by the Air Force Office of Scientific Research, Air Force System Command, USAF, under Contract No. F49620-86-C-0100, and the National Science Foundation, Grant CHE-8318820-02. The United States government is authorized to reproduce and distribute reprints for governmental purposes notwithstanding any copyright notation thereon. We thank Dr. Douglas R. Powell and Professor Lawrence F. Dahl for helpful discussions.

Supplementary Material Available

Structure determination summary for **1** at 22°C, including tables of bond lengths, bond angles, and atomic coordinates (4 pages); tables of H-atom coordinates, anisotropic displacement coefficients, and observed and calculated structure factors for **1** at 22°C and at −100°C (35 pages). Ordering information is given on any current masthead page.

References and Notes

[1] R. West, M.J. Fink, J. Michl, Science, 214, 1981, 1343.

[2] For a recent review, see R. West, Angew. Chem., Int. Ed. Engl., 26, 1987, 1201.

[3] Crystals of tetramesityldisilene grown in toluene incorporate one molecule of solvent per molecule of disilene ($\mathbf{1} \cdot C_7H_8$) [4]. Crystallization in hexane does not integrate solvent in the lattice.

[4] (a) M.J. Fink, M.J. Michalczyk, K.J. Haller, R. West, J. Michl, J. Chem. Soc., Chem. Commun., 1983, 1010. (b) M.J. Fink, M.J. Michalczyk, K.J. Haller, R. West, J. Michl, Organometallics, 3, 1984, 793.

(5) (a) H. Watanabe, K. Takeuchi, N. Fukawa, M. Kato, M. Goto, Y. Nagai, Chem. Lett., 1987, 1341. (b) We have observed that tetra(*ortho*-xylyl)disilene is mildly thermochromic upon heating (bright yellow to light orange).

[6] M. Hesse, U. Klingebiel, Angew. Chem., Int. Ed. Engl., 25, 1986, 649.

[7] P.J. Davidson, D.H. Harris, M.F. Lappert, J. Chem. Soc., Dalton Trans., 1976, 2268.

[8] C. Couret, J. Escudie, J. Satge, M. Lazraq, J. Am. Chem. Soc., 109, 1987, 4411.

[9] K.W. Zilm, G.A. Lawless, R.M. Merrill, J.M. Millar, G.G. Webb, J. Am. Chem. Soc., 109, 1987, 7236.

[10] The monomeric tin amide $[(Me_3Si)_2N]_2Sn$ is also thermochromic; see M.S. Cynone, D.H. Harris, M.F. Lappert, P.P. Power, P. Rivère, J. Rivère-Baudet, J. Chem. Soc., Dalton Trans., 1976, 2004; M.F. Lappert, P.P. Power, Adv. Chem. Ser., 1976, 157, 70.

[11] (a) G. Olbrich, P. Potzinger, B. Relmann, R. Walsh, Organometallics, 3, 1984, 1267; (b) K. Krogh-Jespersen, J. Am. Chem. Soc., 107, 1985, 537; (c) M.S. Gordon, in J.F. Liebman, A. Greenberg, (eds): Molecular Structure and Energetics. Springer-Verlag, New York, Vol. 1, Ch. 4 (1986); (d) M.S. Gordon, T.N. Truong, E.K. Bonderson, J. Am. Chem. Soc., 108, 1986, 1421; (e) H. Teramae, J. Am. Chem. Soc., 109, 1987, 4140; (f) M.W. Schmidt, P.N. Truong, M.S. Gordon, J. Am. Chem. Soc., 109, 1987, 5217.

[12] (a) H. Sakurai, Y. Nakadaira, H. Tobita, T. Ito, K. Toriumi, H. Ito, J. Am. Chem. Soc., 104, 1982, 300; (b) I. Agranat, Y. Tapuhi, J. Am. Chem. Soc., 98, 1976, 615.

[13] There is slight contraction at the lower temperature.

[14] C.N.R. Rao, Ultra-Violet and Visible Spectroscopy. Butterworths, London, 3rd edn., p. 156 (1975).

[15] The twist angle is taken as the dihedral angle between the C–Si–C and C′–Si′–C′ planes.

[16] The pyramidalization is gauged by the angle formed between the C–Si–C plane and the Si–Si vector.

[17] S. Masamune, S. Murakami, J.T. Snow, H. Tobita, D.J. Williams, Organometallics, 3, 1984, 333.

[18] B.D. Shepherd, D.R. Powell, R. West, Organometallics, in press.

[19] A different definition of the twist angle was used in the original report on **1**·C_7H_8 [4].

[20] (a) H. Sakurai, K. Ebata, K. Sakamoto, Y. Nakadaira, C. Kabuto, Chem. Lett., 1988, 965; (b) H. Sakurai, K. Ebata, C. Kabuto, Y. Nakadaira, Chem. Lett., 1987, 301.

[21] For comparison, the rings in planar tetramesitylethylene are inclined at a 53° angle to the C=C plane; J.F. Blount, K. Mislow, J. Jacobus, Act Crystallogr., A, 28 suppl., 1972, S12, abstr. 11-5).

[22] B.D. Shepherd, R. West, Chem. Lett., 1988, 183.

[23] It is likely that the orientation of the aromatic rings in solution is similar to that observed in the solid state.

[24] This long-wavelength absorption is a shoulder on a main band at 338 nm.

[25] (a) H. Watanabe, Y. Kougo, M. Kato, H. Kuwabara, T. Okawa, Y. Nagai, Bull. Chem. Soc. Jpn., 57, 1984, 3019; (b) S. Masamune, Y. Eriyama, T. Kawase, Angew. Chem., Int. Ed. Engl., 26, 1987, 584.

[26] Another derivative, 1,2-di[bis(trimethylsilyl)amino]dimesityldisilene, is red at 22°C in the solid state and in solution λ_{max} = 475 nm [2].